# Photonic Analyses of High Knudsen Number Flows

Tomohide Niimi

*Dept. of Micro and Nano-Systems Engineering, Nagoya University, Furo-cho, Chikusa, Nagoya 464-8603, Japan*

**Abstract.** In late years, the necessity of high Knudsen number flows such as highly rarefied gas flows with large mean free path and gaseous flows around nanodevices with small characteristic length have increased significantly, especially in fields of researches on space technology, surface science, fabrication of thin film for semi-conductor and so on. In this paper, I describe mainly the optical diagnostic techniques for the high Knudsen number flows, such as laser induced fluorescence (LIF), resonantly enhanced multiphoton ionization (REMPI) and pressure sensitive molecular film (PSMF), and our experimental results obtained by the use of the techniques, i.e., applications of LIF to visualization of flow field structures including complicated shock-wave system and to a measurement technique of rotational temperature, establishment of a REMPI system and its application to detection of rotational nonequilibrium in highly rarefied gas flows, and development of the suitable PSMF for low density gas flows.

## INTRODUCTION

To describe the degree of rarefaction, Knudsen number (*Kn*) is defined by the ratio of the mean free path ($\lambda$) divided by the characteristic dimension (L) of the flow. Provided that the *Kn* exceeds 0.01, we cannot approximate the flow as a continuum one, but have to perceive the flow as an atomic or molecular one. We call these flows with large *Kn* "High Knudsen number flows," which correspond not only to low density gas flows with large $\lambda$, but also to gasous flows in micro- or nano-systems with small L. In the case of large $\lambda$, there appear the strong non-equilibrium phenomena because of few intermolecular collisions. For extremely small L, on the other hand, the flow field is strongly influenced by interaction of molecules with a solid boundary rather than intermolecular collisions. Experimental analyses of thermo-fluid phenomena related to the high Knudsen number flows need the optical measurement techniques based on atoms or molecules, such as their emission and absorption of photons. However, the experimental techniques are behind in development compared with the molecular simulation techniques.

In this paper, I mainly introduce laser induced fluorescence (LIF), resonantly enhanced multiphoton ionization (REMPI) and a pressure sensitive molecular film (PSMF), as measurement techniques for high Knudsen number flows. We applied LIF to visualization of flow field structures including complicated shock-wave system [1, 2]and to a measurement technique of rotational temperature [3]. We established the 2R+2 $N_2$-REMPI technique, in which nitrogen molecules are ionized by two steps, i.e., the first step from the ground state to the resonance state (2 photons) and the second step from the resonance state to the ionization state (2 photons). The nitrogen ions are detected as a signal and its spectra depending on the wavelength of an irradiated laser beam are analyzed to measure the rotational temperature through the Boltzmann plot. The 2R+2 $N_2$-REMPI technique is applied to measure the rotational population in supersonic free molecular nitrogen flows and obtain the non-Boltzmann rotational distribution for $P_0 \cdot D$ =15 Torr mm (where $P_0$ is the source pressure and D is the nozzle diameter) [4]. The pressure-sensitive paint (PSP) has potential as a diagnostic tool for pressure measurement in the high Knudsen number regime because the principle of the pressure sensitive paint (PSP) technique is based on oxygen quenching of luminescence [5, 6]. Aiming to apply the PSP to micro devices, we have adopted Langmuir-Blodgett (LB) technique to fabricate pressure sensitive molecular films (PSMFs) using PdOEP and PdMP, and have tested these PSMFs to evaluate the feasibility of the pressure measurement around micro devices [5]. Moreover, the "pressure" distribution obtained by the PSMF is compared with the distribution of the molecular number flux onto the solid surface to investigate its feasibility of number flux measurement [7].

# PHOTONIC ANALYSES OF HIGH KNUDSEN NUMBER FLOWS

## Laser Induced Fluorescence (LIF)

Some atoms and molecules emit fluorescence when irradiated by a laser beam whose wavelength corresponds to an absorption line of molecules. In Fig. 1[1], LIF of iodine molecules ($I_2$) seeded in argon gas visualize a flow field of a supersonic free jet issued from a sonic nozzle with exit diameter of 0.5 mm into a chamber kept at low pressure, clearly showing the Barrel shock waves and Mach disk. We also applied the LIF of $I_2$ to visualization of complicated three- dimensional flowfield structures and shock wave systems of two, three or four interacting supersonic free jets [2].

We proposed a method for planar measurement of temperature in the rarefied gas flows using two-line laser-induced iodine fluorescence in 1990[3]. If the fluorescence intensity at a point in the flow field is designated by $F_1$ when the iodine molecules in the rotational level $J''_1$ are excited and by $F_2$ when the molecules in the level $J''_2$ are excited, the ratio $F_1/F_2$ depends on temperature and two rotational quantum numbers, $J''_1$ and $J''_2$. Therefore, once two absorption lines are selected, the ratio between fluorescence intensities can be expressed as a function of temperature.

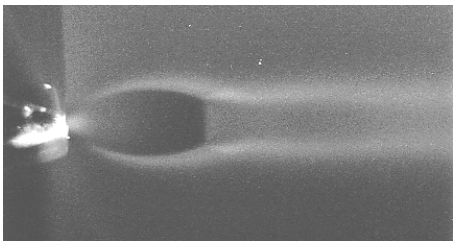

**FIGURE 1.** A Supersonic free jet visualized by $I_2$-LIF

## Resonantly Enhanced Multi-Photon Ionization (2R+2 $N_2$-REMPI)

Supersonic free molecular flows have been utilized to examine temperature nonequilibrium phenomena of diatomic gases[8] and a rotational collision number for rotational relaxation. In these days, a large number of simulation models related to the rotational relaxation have been proposed, which Wysong and Wadsworth [9] reviewed in detail for a DSMC (direct simulation Monte Carlo) method.

Using an electron beam fluorescence method developed by Muntz[10], Marrone[11] measured a rotational temperature distribution quantitatively along the centerline of a supersonic nitrogen free jet, adopting the $P_0D$ (depending inversely on the nozzle Knudsen number; $P_0$: source pressure, $D$: orifice diameter) as a parameter. These experimental data obtained in 1967 have been employed to verify the simulation data. However, the rotational distributions measured by Marrone deviated from Boltzmann distributions, especially on the higher rotational energy states. Although the rotational distribution shows nonlinearity in the Boltzmann plot, he described in his paper that the nonlinearity was caused by secondary electrons. On the contrary, Coe et al.[12] proposed a new analytical model including a quadrupole interaction with an ejected electron as well as a dipole interaction with a primary electron and reduced the spectroscopic data to the Boltzmann distribution successfully, concluding that there were no deviation from the Boltzmann distribution in the rotational states in wider range of $P_0D$ from 15.9 to 1016 Torr-mm. Only recently, the quantum mechanics has been introduced to numerical simulations and the non-Boltzmann distribution in the rotational levels has been discussed actively. Koura[13] developed a new calculation method combined the DSMC and CTC (classical trajectory calculation) methods and indicated the non-Boltzmann rotational distribution of nitrogen gas expanding spherically. Unfortunately, he was still comparing the simulation data with Marrone's results, which are the only experimental data for researchers studying the rotational relaxation. Because there have been no experimental data of the rotational energy distributions since the experiments by Marrone[11] and Coe et al.[12], we desire the precise experimental data earnestly using the laser spectroscopy.

In the present study, we measure the rotational population in supersonic nitrogen free jets using a REMPI (Resonantly Enhanced Multi-Photon Ionization) method, detecting nitrogen ions directly as an ion current. In the REMPI method, photon energy is reduced to one-fourth compared with the electron beam fluorescence method, because nitrogen molecules are ionized by four photons. This means that the ejected electrons by photons excite no other molecules or ions again, leading to no consideration of the secondary electrons for spectral analyses. Furthermore, unlike the electron beam method using fluorescence emitted by ions transferred from an excited state

($N_2^+B^2\Sigma_u^+$) to a ground state ($N_2^+X^2\Sigma_g^+$), the REMPI spectrum reflects the rotational population in the ground state of neutral molecules directly. We apply REMPI to the supersonic nitrogen free jets with $P_0D$ of 15 Torr-mm or lower, the lowest value of the experiments of Marrone, and confirm the non-Boltzmann distribution of the rotational levels experimentally.

Figure 2 depicts the schematic energy level diagram (illustrating the relevant processes) for 2R+2 $N_2$-REMPI. In this process, nitrogen molecules at the ground state ($X^1\Sigma_g^+$) are excited to the resonant state ($a^1\Pi_g$) by two-photon absorption. Then the excited molecules are ionized by additional two-photon energy. Because four photons participate in this process, the ion current is proportional to the fourth power of laser flux when the flux is relatively low. On the other hand, when the laser flux is sufficiently high so that almost all the excited molecules ionize, the ion current is proportional to the second power of laser flux, because the REMPI process reflects the two-photon transition process from the ground to the resonant state. In this case, since the REMPI spectra depend on the rotational energy distribution at the ground state, the rotational temperature can be deduced from the REMPI spectra, provided that the flow is in equilibrium. In the 2R+2 $N_2$-REMPI method, photon energy for ionization of nitrogen molecules is reduced to one-fourth compared with the electron beam method, in which nitrogen molecules are directly ionized by one electron. This means that for the 2R+2 $N_2$-REMPI, the electrons ejected by photons excite no other molecules or ions again, leading to no consideration of the secondary electrons for spectral analyses. Furthermore, unlike the electron beam method detecting fluorescence emitted by ions transferred from an excited state of the molecular ion ($N_2^+B^2\Sigma_u^+$) to a ground-state ion ($N_2^+X^2\Sigma_g^+$), the REMPI spectrum reflects the rotational population in the ground state of neutral molecules directly.

As shown in Fig. 3, all experiments are carried out in the vacuum chamber evacuated by a 2300ℓ/sec turbomolecular pump (ULVAC UTM-2300FW) and a dry pump (ULVAC LR90) as a backing pump, allowing an oil-free vacuum environment. Nitrogen gas is issued from a sonic nozzle with a $D$=0.50 mm diameter, and expanded into the chamber. Stagnation temperature is kept at 293K. We set stagnation pressures $P_0$ at 30 Torr (3999 Pa), 20 Torr (2666 Pa), 10 Torr (1333 Pa) and 1 Torr (133.3Pa) which result in background pressure $Pb$ of 1.0 $\times 10^{-3}$ Torr ($1.3 \times 10^{-1}$ Pa), $7.5 \times 10^{-4}$ Torr ($1.0 \times 10^{-1}$ Pa), $4.0 \times 10^{-4}$ Torr ($5.3 \times 10^{-2}$ Pa), $3.3 \times 10^{-5}$ Torr ($4.4 \times 10^{-3}$ Pa), respectively. A Nd:YAG-pumped dye laser (Lambda Physik, SCANMATE OG 2E C-400) operated with Rhodamine 6G dye is used as a laser source, and the output is frequency-doubled by a BBO crystal. The wavelength of the laser beam is ranged from 283 to 284.1nm. The beam is focused with a quartz lens (f = 120mm) on a centerline of a nitrogen free-molecular flow. The energy, repetition rate, and duration time of the laser beam are 7.0 mJ/pulse, 10 Hz, and 6 ns, respectively. The ionized nitrogen molecules are detected by a secondary electron multiplier (Murata, CERATRON EME-2061C) for stagnation pressure of 1 Torr and a tungsten Langmuir probe with a 0.05 mm diameter and a 1.5 mm length, on which – 2.0 kV is applied, for the pressure of 10 Torr or higher. The signal intensity is recorded on a personal computer after amplified by a current-input preamplifier (NF, As-905-1, gain: $4\times10^6$ V/A) and averaged by a boxcar integrator (STANFORD RESEARCH SYSTEM, SR250, SR245 and SR280). A wavelength is scanned by a step of 0.001nm, and the signal intensity is integrated for 100 laser pulses per each step.

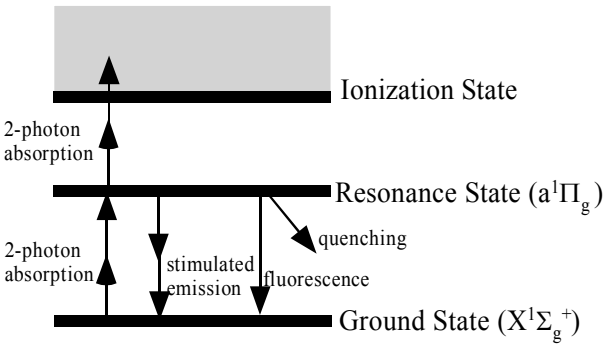


**FIGURE 2.** 2R+2 $N_2$-REMPI process

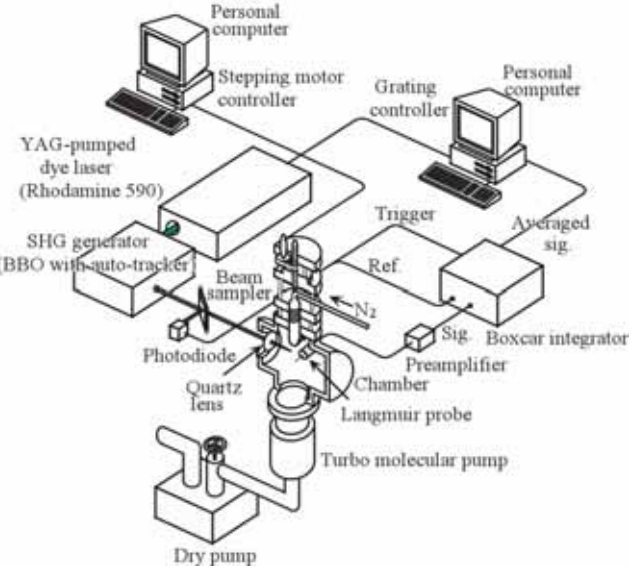


**FIGURE 3.** Experimental apparatus

Figure 4 represents an experimental 2R+2 $N_2$-REMPI spectrum of the ($v'$, $v''$ ) = (1, 0) band, measured for $P_0D$ =15 Torr-mm and at a focal point of $x$=2.5 mm downstream from the nozzle exit (x/$D$ =5) along the centerline of the jet. In this figure, the horizontal axis indicates the wavelength of the laser, and the vertical one the signal intensity normalized by a peak. Numbers on rulers in the figure correspond to spectral positions for O, P, Q, R and S branches.

When the population number is designated by $N(J'')$, the rotational line intensity $I_{J',J''}$ in 2R+2 $N_2$ -REMPI spectra is given by

$$I_{J',J''} = Ag(J'')S(J',J'')N(J'')/(2J''+1),$$

where $J'$ and $J''$ are the rotational quantum number of the resonant and ground state, respectively, $A$ is a proportional constant independent of the rotational quantum numbers, $g(J'')$ is the nuclear spin statistical weight of nitrogen molecules formed by $N^{14}$ atoms, whose value is 3 and 6 for odd and even $J''$, respectively. $S(J',J'')$ is the two-photon Hönl-London factor[14] for the $a^1\Pi_g \leftarrow X^1\Sigma_g^+$ transition. $N(J'')$ is proportional to $(2J''+1)\exp(-E_{rot}/kT_{rot})$, provided that the rotational energy distribution follows the Boltzmann distribution. In this case, $I_{J',J''}$ is given by[8]

$$I_{J',J''} = Ag(J'')S(J',J'')\exp(-E_{rot}/kT_{rot}),$$

and the rotational temperature can be deduced by a slope of Boltzmann plot of $\ln(I_{J',J''}/gS)$ versus $E_{rot}/k$, provided to be in equilibrium. If there appears nonlinearity in the Boltzmann plot, therefore, the rotational energy distribution deviates from the Boltzmann distribution and the rotational temperature cannot be defined.

Figure 5 shows a result of Boltzmann plots at several $x/D$'s for $P_0D$ =15 Torr-mm by using the measured REMPI spectra. In this figure, the horizontal axis indicates the $E_{rot}/k$ and the vertical one the $\ln(I_{J',J''}/gS)$. Numbers attached to the data points are the rotational quantum numbers of the ground state.

It is found from Fig. 5 that all the Boltzmann plots demonstrate the nonlinearity even at $x/d$=1.0 for $P_0D$ =15 and especially the data in higher rotational levels deviate from a line, confirming the non-Boltzmann distribution of the rotational levels. Furthermore, it is also clarified that deviation from the line starts at a smaller rotational level as the flow proceeds downstream, i.e. as $x/D$ becomes larger. We found that the influence of the background gas molecules on the rotational energy distribution of the free molecular jet is negligibly small [4].

In the same way as Marrone, we obtained the rotational temperature by using only the linear portion of the plots lying at smaller rotational quantum numbers. Figure 6 shows the rotational temperature distribution along the centerline of a supersonic free jet, measured by Boltzmann plots of Fig. 5. In these figure, the horizontal axis indicates $x/D$ and the vertical one the rotational temperature. Solid circles indicate the measured rotational temperatures, and the broken lines the translational temperature distribution, calculated from isentropic relations using the Mach numbers given by Ashkenas and Sherman[15]. The rotational temperature distribution for $P_0D$ =15 (Fig. 6) measured by using the REMPI is also compared with that obtained by Marrone and the both agree well with each other. Marrone also measured the rotational temperature using only some rotational lines constituting a part of non-Boltzmann distribution, describing in his paper that the nonlinearity might be a measurement error caused by secondary electrons. However, since our results obtained by REMPI, which is not influenced by the secondary electrons, also show the nonlinearity in the Boltzmann plots, it is evident that the non-Boltzmann distribution of the rotational levels appears in the supersonic free molecular nitrogen flows even at $P_0D$=15 Torr-mm. Gallagher and

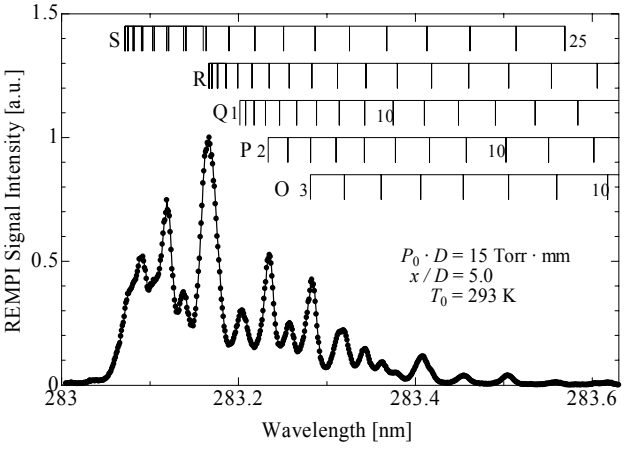


**FIGURE 4.** 2R+2 $N_2$-REMPI spectrum for $P_0D$ =15 Torr-mm and at x/$D$ =5

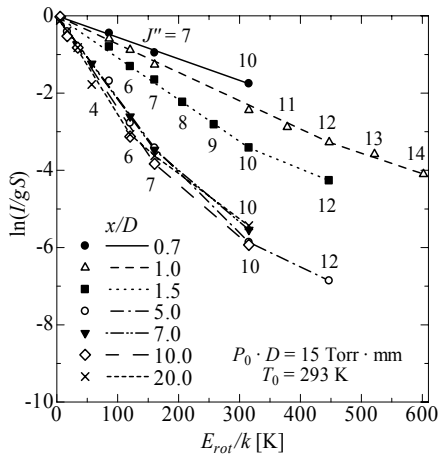


**FIGURE 5.** Boltzmann Plots ($P_0D$ =15 Torr-mm)

Fenn[16] derived an equation of the rotational temperature distribution along the centerline of a supersonic free jet, which has a rotational collision number $Z_R$ for the rotational relaxation as an only parameter depending on the kind of gas. The rotational temperature distribution calculated by this equation is also depicted in Fig. 6 and agrees well with Marrone's and our results only for $Z_R$=1.3, though Wysong and Wadsworth[9] reviewed about $Z_R$ strongly depending on temperature.

To clearly reveal the non-Boltzmann distribution, the rotational population obtained by REMPI for $P_0D$=15 is presented in Fig. 7, in which the horizontal axis indicates the rotational quantum number and the vertical one the population ratio for each rotational level to the total. Symbols such as solid circles correspond to the population ratio for each measurement point and each curve to a Boltzmann distribution at temperature deduced by Boltzmann plot using only the data for smaller rotational quantum numbers as mentioned above. In the condition of $P_0D$=15 Torr-mm, at $x/d$=1.0 the rotational population follows almost the Boltzmann distribution, whereas at $x/d$=7.0 the experimental data deviate from the Boltzmann distribution evidently. Comparing between the distributions of $x/d$=7.0 and 20.0, for $J''\geq 7$ the both show the same tendency, suggesting partial freezing of the rotational population. Generally the higher rotational quantum number the molecules have, the lower the transition probability becomes, resulting in the deviation from the Boltzmann distribution particularly for the higher rotational levels. This is the reason why the freezing of the rotational population starts partially at the higher rotational levels.

On the other hand, for $P_0D$=5.0 Torr-mm, we can find the deviation from the Boltzmann distribution even at $x/d$=1.0, in which for $J''\leq 10$ the population is consistent with the Boltzmann distribution, but for $J''\geq 11$ the population becomes higher than it. At $x/d\geq 2.0$, furthermore, the deviation starts at the lower rotational levels, i.e. $J''\geq 7$. By comparison of $x/d$=2.0 with 3.0, the both distributions approximately coincide with each other, so that we believe that the rotational population freezes in the vicinity of $x/d$=2.0.

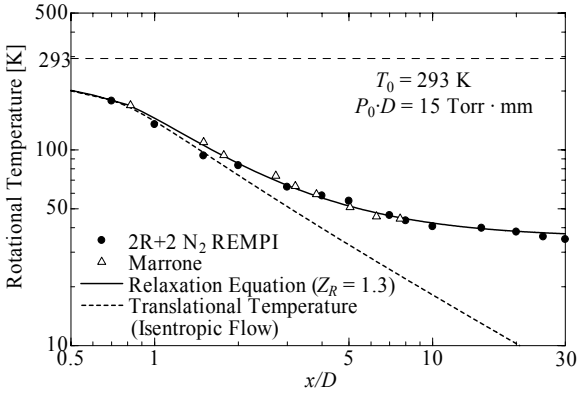


**FIGURE 6.** Rotational temperature distributions along the centerline of the jet ($P_0D$ =15 Torr-mm)

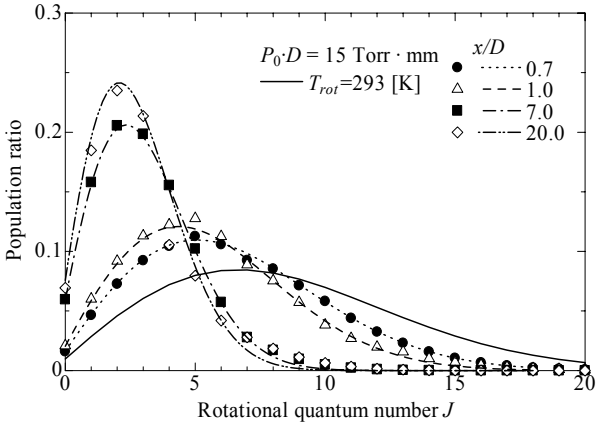


**FIGURE 7.** Rotational populations ($P_0D$ =15 Torr-mm )

## Pressure Sensitive Paints

Experimental analyses of thermo-fluid phenomena with high Knudsen number, related to low density gas flows or nano-technologies, need the measurement techniques based on atoms or molecules, such as emission and absorption of photons. However, the techniques are behind in development compared with the molecular simulation techniques. In the case of gas flows inside the micro-systems, measurement of pressure on the surfaces has almost never been reported and development of its measurement technique has been eagerly anticipated. Of course, it is not realistic to apply pressure taps to micro-systems, because dimensions of typical pressure taps are comparable to those of micro-systems.

The sensitivity of PSPs depends mainly on the quenching probability of the luminophore as well as the oxygen permeability of the binder. In the previous study [5-7], we have clarified that a glassy polymer poly(TMSP) with extremely high oxygen permeability is suitable as a binder of PSP for low-pressure condition, because poly(TMSP)-based PSP shows very high pressure sensitivity and no hysteresis property. To increase the pressure sensitivity further, luminophore with high quenching probability should be selected. In this study, we have tested three kinds of porphyrins to select the suitable luminophore. One of the luminophores is PtTFPP, which has been commonly used as a luminophore of PSP, and the others are palladium porphyrins, PdOEP and PdTFPP. We have examined their

fundamental properties such as pressure sensitivity and temperature dependence of luminescence intensity in the range of pressure below 1 Torr. Moreover, the pressure distribution on a small solid surface interacting with a low-density supersonic free jet is measured by the PSP, showing the applicability of PSP to high Knudsen number conditions.

The pressure measurement technique using PSP is based on oxygen quenching of luminescent molecules[17,18]. A PSP is composed of luminescent molecules and a binder material to fix the luminescent molecules to a solid surface. When the PSP layer painted on the surface is irradiated by UV light, the luminescent molecules at the ground singlet state can be excited by absorption of photon energy to a higher singlet state. After the transition of the excited molecules from the singlet state to the lowest triplet state by an intersystem crossing, the molecules emit phosphorescence and transfer to the ground singlet state. Because the transition between the triplet state and the singlet state is spin forbidden, the lifetime of the phosphorescence is long. On the other hand, oxygen molecules, whose ground state is triplet, act as a quencher of the luminescence. As a result, the phosphorescence intensity decreases as an increase in partial pressure of oxygen. Pressure on the solid surface can be deduced from the relationship between pressure and the luminescence intensity called as Stern-Volmer plot [18].

$$\frac{I_{ref}}{I} = A_0 + A_1 \frac{P}{P_{ref}}. \tag{3}$$

where $I$ is the luminescence intensity and and P is the oxygen pressure. $I_{ref}$ is the luminescence intensity at the known reference pressure $P_{ref}$. $A_n$ are the constants called as Stern-Volmer coefficients determined by calibration tests. $I_{ref}/I$ depends linearly on $P/P_{ref}$ following to Eq. (3), but the actual PSPs have nonlinear dependence of $I_{ref}/I$ on $P/P_{ref}$. Therefore, the following equation considering the nonlinearity should be employed:

$$\frac{I_{ref}}{I} = \sum_{n=0}^{N} A_n \left( \frac{P}{P_{ref}} \right)^n. \tag{4}$$

In practice, a second-order polynomial ($N = 2$) is commonly used. It should be noted that the coefficients $A_n$ have the dependence on the temperature of the solid surface, because both the quenching probability of luminescent molecules and the oxygen permeability of binder depend on temperature. Therefore, the effect of the temperature must be eliminated for precise measurements

Figure 8 shows the experimental apparatus composed for this study. The PSPs are painted on aluminum plates (50 mm × 25 mm) by an airbrush and then the plates are set inside a vacuum chamber evacuated by a scroll pump (ULVAC DVS-631) and a turbo molecular pump (ULVAC UTM-300). Oxygen gas is supplied into the chamber through a pressure control valve, and the pressure is monitored by a capacitance manometer and an ionization vacuum gauge. The temperature of the PSP sample is controlled by a Peltier thermo-controller and is monitored by a thermocouple. A xenon-arc lamp with a band-pass filter is used as an excitation light source, and the light is transmitted via an optical fiber. The wavelength range of the band-pass filter is 400 ± 20 nm. The luminescence is filtered by a short-cut filter (600 nm) to eliminate the light from the xenon lamp, and is detected by a CCD camera with an

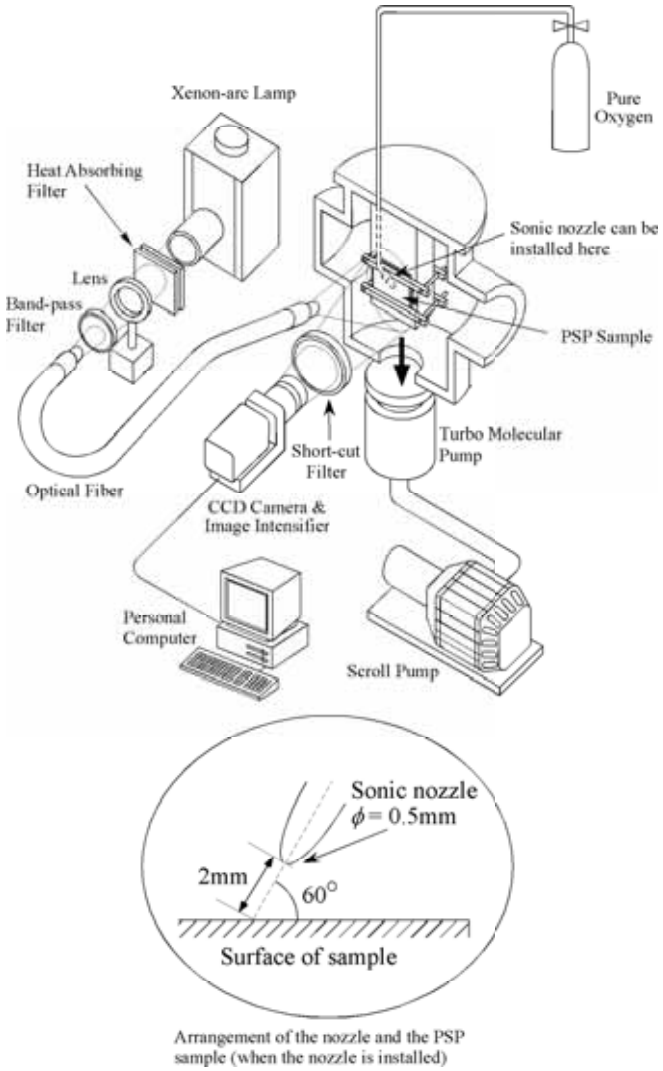


**FIGURE 8.**. Experimental apparatus for PSP

image intensifier. The image of the luminescence is processed by a personal computer.

Figure 9 shows the Stern-Volmer plot of PSPs using poly(TMSP) as a binder against oxygen pressure. The reference pressure $P_{ref}$ was $1.0\times10^{-2}$ Pa for (a) and $1.3\times10^{2}$ Pa for (b), and the temperature $T$ was kept at 300 K for the both cases. As easily seen in Fig. 9(a), both PdOEP and PdTFPP have extremely high pressure-sensitivity in the low-pressure condition below 130 Pa. However, the pressure sensitivity of PdOEP and PdTFPP in the relatively high pressure above 130 Pa decreases gradually as shown in Fig. 9(b), showing the strong nonlinearity of the Stern-Volmer plots. Because the luminescence of both PdOEP and PdTFPP is highly quenched and saturated at the pressure above 130 Pa, the dependence of the luminescence intensity on the oxygen pressure disappears. As a result, PdOEP and PdTFPP bound by poly(TMSP) would be very powerful measurement tools in the low pressure condition below 130 Pa, although they cannot be applied in the higher pressure range. The result implies that the two PSPs can be applied to microsystems.

As an application of PSP in a high Knudsen number condition, PdOEP bound by poly(TMSP), having very high sensitivity in low pressure conditions, was applied to measure pressure distributions on an aluminum plate interacting with a supersonic free jet. The arrangement of the jet and the plate is depicted in Fig. 8. Oxygen was used as a test gas for the experiments, and the source pressure $P_s$ was set at 1300 Pa and 130 Pa. The resulting background pressure $P_b$ was 1.3 Pa and $7.6\times10^{-2}$ Pa, respectively.

Figures 10(a) and (b) show the pressure distributions measured by the PSP, for $P_s$ = 1300 Pa and 130 Pa, respectively. In the pictures, 1 mm over the surface corresponds to 57 pixels of the images obtained by the CCD camera, indicating the spatial resolution of the images is 18 μm. The images do not indicate the luminescence intensity distributions themselves, but the calibrated two-dimensional pressure distribution maps clearly; white color corresponds to high-pressure regions and black color to low-pressure regions.

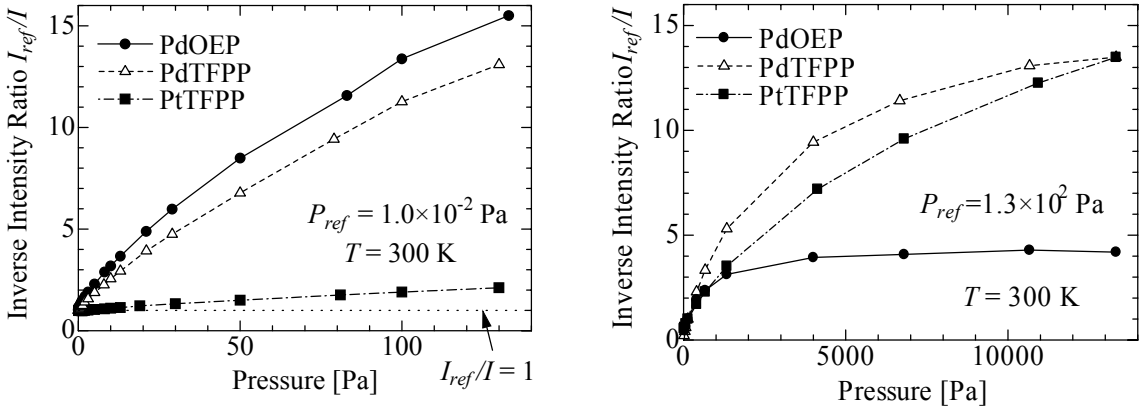


(a) Low pressure condition (b)High pressure condition

**FIGURE 9.** Stern-Volmer plots for three types

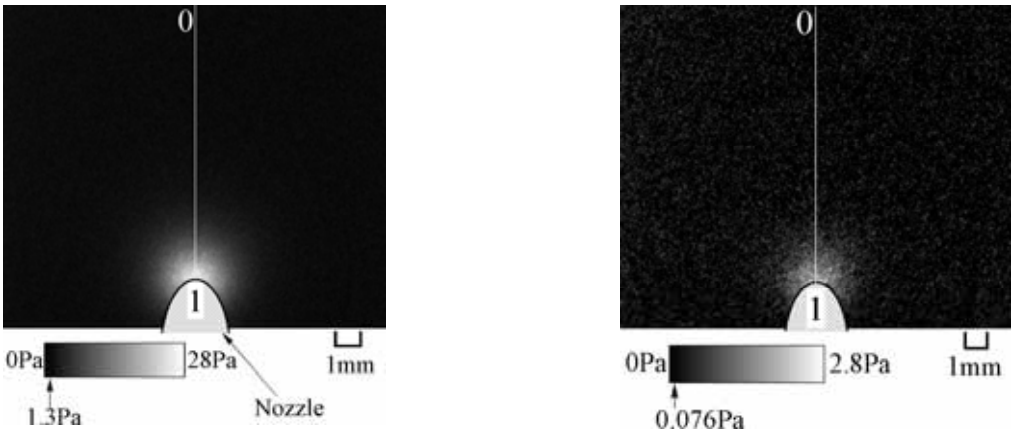


(a) $P_0$ = 1.3×10$^3$ Pa (10 Torr) (b) $P_0$ = 1.3×10$^2$ Pa (1 Torr)

**FIGURE 10.** Pressure distribution measured by PdOEP

Because the PSP technique utilizes quenching of the luminescent molecules by oxygen molecules, it seems suitable for analyses of high Knudsen number flows, which require diagnostic tools in the molecular level. However, application of the PSP technique to a micro-system is very difficult, because the layer of a conventional PSP is too thick owing to the use of polymer binder, and the aggregation of luminescent molecules cause low spatial resolution. In this study, we have adopted Langmuir-Blodgett (LB) method to fabricate a pressure sensitive molecular film (PSMF) applicable to pressure measurement around micro-devices. Because the LB method can construct ordered molecular assemblies, a PSMF with nanometer order thickness and high spatial resolution seems suitable for analyses of micro-flows.

Our research group has applied PdMP, one of the amphiphilic palladium porphyrins, as a luminophore of the PSMF, because amphiphiles can form stable LB films. Figure 11 shows the Stern-Volmer plots for PSMFs of 2-layer, 6-layer and 20-layer in the pressure condition below $1.3\times10^{2}$ Pa. The horizontal axis of each Stern-Volmer plot is the pressure $P$, the vertical axis is the inverse luminescent intensity ratio $I_{ref}/I$, where the $I_{ref}$ is the luminescence intensity at the reference pressure $P_{ref}=1.0\times10^{-2}$ Pa. It is shown that the PSMF of PdMP has sufficient pressure sensitivity in the low pressure region with high Knudsen number, even if the amount of the luminescent molecules in PSMF layer, whose thickness is in the order of nanometer, is much smaller than that in conventional PSPs, whose thickness is in the order of micron. It is found that the presssure sensitivity of PSMF composed of PdMP is higher than that of PSMF composed of PdOEP.

The sensitivity of the 2-layer PSMF is higher than that of the 6-layer and the 20-layer PSMFs. It is because the change of luminescence intensity is almost equal regardless of the number of layers. The fact indicates that the oxygen molecule only interacts with the outermost layer, that is, oxygen quenching occurs at the outermost layer only. For the further improvement of pressure sensitivity, it is important to improve the oxygen permeability of the PSMFs.

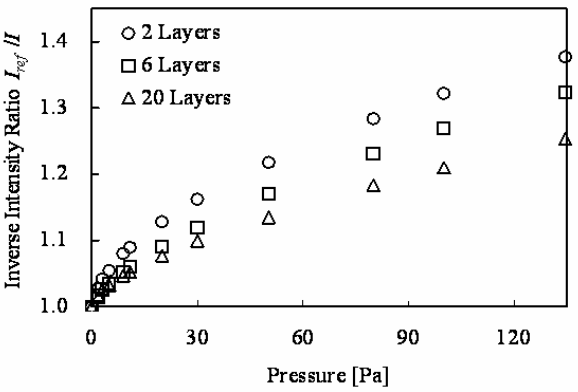


**FIGURE 11.** Stern-Volmer plot for PSMF of PdMP

## ACKNOWLEDGMENTS

The present work was supported by a grant-in-aid for Scientific Research from the Japanese Ministry of Education, Science and Culture.

## REFERENCES

1. T. Fujimoto and T. Niimi, Rarefied Gas Dynamics, Space-Related Studies, AIAA(1988), pp. 391-406.
2. T. Niimi, T. Fujimoto and N. Taoi, JSME Int. J. , B, 39, 1(1996), 95-100.
3. T. Niimi, T. Fujimoto and N. Shimizu, Proc. 17th Int. Symp. on Rarefied Gas Dynamics, VCH, (1991), pp. 1482-1489.
4. H. Mori, T. Niimi, I. Akiyama and T. Tsuzuki, Physics of Fluids, 17(11), 117103(2005).
5. T. Niimi, et al., J. of Thermophysics and Heat Transfer, AIAA, Vol.19, No.1, pp.9-16 (2005).
6. H. Mori, T. Niimi, M. Hirako and H. Uenishi, Meas. Sci. Technol., 17, 1242(2006).
7. H. Mori, T. Niimi, M. Hirako and H. Uenishi, Physics of Fluids, **17**(10), 100610 (2005).
8. Niimi, T., Proc. of 23rd Int. Symp. on Rarefied Gas Dynamics, AIP, Vol.663(2002), pp. 1025-1032.
9. Wysong, I. J. and Wadsworth, D. C., Phys. Fluids, 10, 11, 1998, pp. 2983-2994.
10. Muntz, E. P., Phys. Fluids, 5, 1, 1962, pp. 80- 90.
11. Marrone, P. V., Phys. Fluids, 10, 3, 1967, pp. 521-538.
12. Coe, D., Robben, F., Talbot, L. and Cattolica, R., Phys. Fluids, 23, 4, 1980, pp. 706-714.
13. Koura, K., Phys. Fluids, 14, 5, 2002, pp. 1689-1695.
14. Bray, R.G. and Hochstrasser, R.M., Mol. Phys., Vol.31, No.4 (1976), pp.1199-1211.
15. Ashkenas, H. and Sherman, F.S., Proc. of 4th Int. Symp. on Rarefied Gas Dynamics, Vol.2 (1966), pp.84-105.
16. Gallagher, R. J. and Fenn, J. B., J. Chem. Phys., 60, 9, 1974, pp. 3487-3491.
17. R. H. Engler, K. Hartmann, I. Troyanovski, and A. Vollan, DLR-FB 92-4, DLR (1991).
18. T. Liu, B. T. Campbell, S. P. Burns, and J. P. Sullivan, Appl. Mech. Rev., **50**, 4, pp. 227-246 (1997).